2021 43rd Annual International Conference of the
IEEE Engineering in Medicine & Biology Society (EMBC)
Oct 31 - Nov 4, 2021. Virtual Conference

Spatial Detection of the Shafts of Fractured Femur for Image-Guided Robotic Surgery*

Marzieh S. Saeedi-Hosseiny, Fayez Alruwaili, Akash S. Patel, Sean McMillan, Iulian I. Iordachita, *Senior Member, IEEE*, Mohammad H. Abedin-Nasab

***Abstract*— Femur fractures due to traumatic forces often require surgical intervention. Such surgeries require alignment of the femur in the presence of large muscular forces up to 500 N. Currently, orthopedic surgeons perform this alignment manually before fixation, leading to extra soft tissue damage and inaccurate alignment. One of the limitations of femoral fracture surgery is the limited vision and two-dimensional nature of X-ray images, which typically guide the surgeon in diagnosing the position of the femur. Other limitations include the lack of precise intraoperative planning and the process of trial-and-error alignment. To alleviate the issues discussed, we develop a marker-based approach for detecting the position of femur fragments using two X-ray images. The relative spatial position of the femur fragments plays a key role in guiding an innovative robotic system, named Robossis, for femur fracture alignment surgeries. Using the derived three-dimensional data, we simulate pre-programmed movements to visualize the proposed steps of the alignment method, while the bone fragments are attached to the robot. Ultimately, Robossis aims to improve the accuracy of femur alignment, which results in improved patient outcomes.**

I. Introduction

One-third of all fractures come from lower limb injuries, among them 430,000 femur fractures annually in the US [1], [2]. Surgery used to treat these fractures is often strenuous, partly limited by the two-dimensional quality and field of view by intra-operative X-rays, and by the high forces required to realign bone fragments. Consequently, 28% of patients experience rotational malalignment of 15° or more after femur fracture fixation [3], [4], who then need additional follow-up surgery with increasing costs and risk of complications.

The integration of robotic assistance and 3D-image guidance has considered to be a promising solution to overcome these surgical issues [5]. Tang *et al*. proposed a 3D-CT-image-reconstruction-based hexapod computer-assisted fracture reduction system for long bone diaphyseal fractures. Similarly, Wang *et al.* developed a parallel robot on a traction table using 3D images [6]. The feasibility of using CT scans for image-guided navigation was explored in [7]. Although extensive work has been reported in [5] demonstrating the efficacy, superiority, and safety of image-guided robotic assistance in orthopedic surgeries, surprisingly few systems are available for femur fracture alignment.

The traditional operating room for femur fracture alignment is often equipped with a C-arm, a fluoroscopic X-ray imaging machine. Thus, there is a major advantage of using the current setting without adding extra cameras and/or CT scan devices to provide 3D information necessary for robot-assisted surgeries, which is the focus of this paper. A review of current literature provides an ample number of studies on 2D to 3D transformation from X-ray images. Baka *et al.* proposed a method to reconstruct distal femur using statistical shape modeling [8]. Zachow offered an algorithm to compare the virtual X-ray images to the reference X-rays, which evaluates their intensity distribution. Using this method, he defined a 3D reconstruction method for bone, using two X-ray images [9]. Laplacian surface deformation for template reconfiguration was studied by Karade and Ravi for 3D bone reconstruction from two X-ray images [10]. While these methods have shown accurate results in 3D reconstruction, they either require a large database or a prior 3D template model. An alternative method that achieves comparable precision without such dependence would be desirable.

Motivated by these remarks, this paper introduces an innovative robotic system, called Robossis, for femur fracture alignment, where a marker-based approach is proposed to derive the relative spatial positions of the distal and proximal

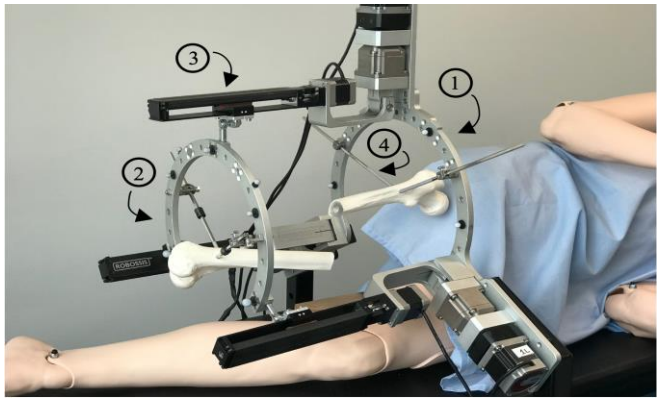

Figure 1. Robossis is a 3-armed wide-open parallel robot for femur fracture alignment surgery. The mechanism consists of (1) a fixed platform, (2) a moving platform, and (3) three arms. (4) half-pin rods to attach the rings to the fractured bone.

*This research is partially funded by the National Science Foundation (NSF) under grant 2005570 and by the New Jersey Health Foundation (NJHF) under grant PC 62-21.

M. S. Saeedi-Hosseiny is with the Electrical and Computer Engineering Department, Rowan University, Glassboro, NJ 08028, USA (e-mail: saeedi64@rowan.edu).

F. Alruwaili, A. Patel, and M. H. Abedin-Nasab are with the Biomedical Engineering Department, Rowan University, Glassboro, NJ 08028, USA (e-mail: alruwa16@rowan.edu, patela67@students.rowan.edu, corresponding author's email: abedin@rowan.edu).

S. McMillan is with Rowan University School of Osteopathic Medicine, Stratford, NJ 08084, and Virtua Health System, Willingboro, NJ 08046, USA (e-mail: smcmillan@virtua.org).

I. I. Iordachita is with the Laboratory for Computational Sensing and Robotics, Johns Hopkins University, Baltimore, MD 21218, USA (e-mail: iordachita@jhu.edu).

femur fragments from two intraoperative X-ray images, to provide a vision for Robossis. As a marker, a coin with a known shape and size is placed in the scene near the femur fragments during C-Arm's operation. Instead of using bone surface, the main femur landmarks are engaged together with the marker for 2D to 3D triangulation. The spatial position of the principal axes of the femur fragments provides the basic information needed to guide the Robossis to align the bone along a predetermined path. Using the proposed robotic system, we can use the path-planning algorithm to achieve the desired results with less potential for human error. The rest of the paper is as follows; Section II overviews the design features of Robossis, Section III focuses on the proposed marker-based approach, and Section IV presents the preliminary experimental results, followed by the conclusion in Section V.

II. Surgical Robot

Long bone fracture alignment has been an area of interest for robotic application due to its ability to achieve greater control and accuracy than the traditional method to improve patient outcomes. Prior to 2008, serial robotic arms were tested to measure their aptitude for fracture reduction [11], [12]. Recently, however, parallel robots have been the preferred model for achieving fine positioning and stability with high load-carrying capacity. Notably, the 6-armed Gough-Stewart robot has been the focus of study for fracture reduction [5]. However, its limited workspace and obstruction of the surgeon's vision due to the number of arms restrict practical application for fracture reduction surgeries [13]. To address these issues, a new 3-armed parallel robot, called Robossis, is designed to achieve complete success [14]. Using active joints, Robossis has been able to have half the number of arms compared to its predecessor. This decrease reduces interference between kinematic chains and expands the robot's workspace, thus providing the ability to align the fracture [15].

The structural components of Robossis, as shown in Figure 1, include a fixed plate that provides an anchor for the robot, a moving plate that acts as the end-effector, and three arms that provide support for maneuverability. Each of these arms has a universal, prismatic and spherical joint. During operation, two rods are employed to fix bone fragments to each respective platform. Accordingly, the 3-armed robot can expend a large amount of power through these rods to deliver enough counteractive force against muscle resistance. The design of Robossis provides superior accuracy, power, and workspace accessibility for the surgeon, however, this robot needs vision. In the next section, we introduce a marker-based approach to provide a vision for Robossis.

III. Marker-Based Detection of Femur Shaft in Space

Robossis can manipulate the main femur fragments in a predetermined trajectory with low speed and high accuracy [14]–[16]. Determining the initial relative position of femur fragments is essential to derive such a trajectory. The current standard to acquire the spatial location of the femur fragments in the traditional operating room is taking several X-ray images, while the manual bone manipulation is in progress by the surgeon. Doing so causes health risks to patients and medical staff in the operating room due to high radiation exposure. Because Robossis motion is precisely measurable

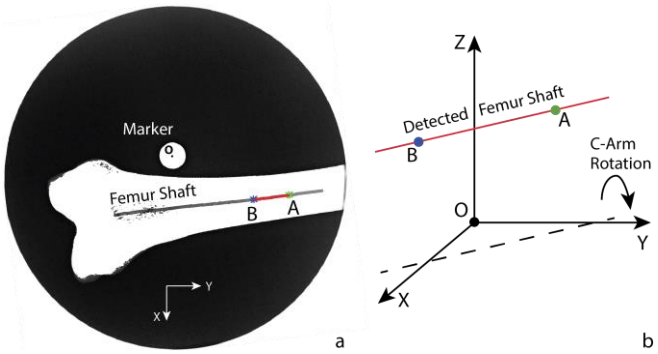

Figure 2. (a) Detected distal femur shaft and the marker in the X-ray image. (b) Schematic view of the detected main femur axis in the XYZ coordinate. The marker center is defined as the origin of the global coordinate.

and traceable, the system only needs the initial and final positions of the proximal and distal parts to move the bone along a predetermined path. With these valuable robot capabilities, the number of required X-ray images is reduced from 100 images to less than 10 images. We know that anatomical alignment is the final desirable condition. To obtain the relative initial position of the femur fracture, this section proposes a marker-based visual approach. Descriptive symbols are selected as the defining points of 2D to 3D conversion. When X-rays are taken, a coin is placed near the bone to act as a triangulation marker (Fig. 2.a).

Section III. presents the detection of femur main landmark in the X-ray images. To define the required setup for 3D positioning of the detected landmarks, we explain the procedure of identifying the local and global coordinates in Section III.B. Using the detected landmarks and the corresponding coordinates, the relative spatial position of the main femur fragments is derived in Section III.C.

A. Landmark detection

Anatomical landmarks, the biologically specific locations on the bone, are proper key points that enable correlation across domains in X-ray images [17]. Thus, the main shaft of the femur is considered a strong constraint for the bone position. Several fundamental image processing algorithms are used to detect the centerline of the femur, which serves as the key feature for the 2D to 3D transformation. For the sake of clarity, the technical details of these algorithms have been omitted and can be found in [18]. To focus on the desired area in the image, we first use a circular mask for each X-ray image. Then, using the connected components, we segment the bone from the background. We use some morphological operations to retrieve incorrect segmentations. Finally, the centerline of the femur is found via skeletonization (Fig. 2.a).

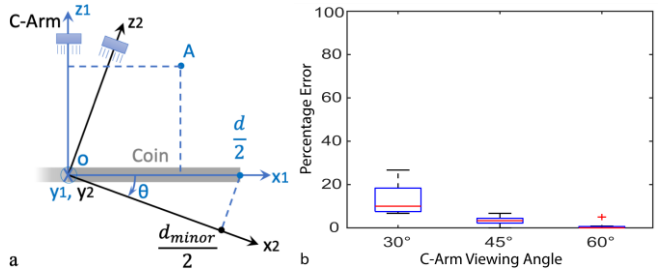

Figure 3. (a) Demonstration of the relative coordinate for each X-ray image, while the C-Arm viewing angle is changing. "O" is the coin center. (b) The percentage error of the C-Arm rotation angle was calculated based on the detected marker diameters.

B. Global coordinate

To have a trusted correlation between images, independent of the C-Arm viewing angle, we define a global coordinate system. To this end, we locate a marker (coin) in the scene, near the bone, while the C-Arm rotates around the bone and takes 2 required X-ray images from 2 arbitrary viewing angles. We develop an algorithm to determine the major and minor diameters of the marker projection in X-ray images. Then, the scaling ratio and the origin of the global coordinates are defined. Therefore, 2D to 3D transformation is possible (Fig. 2.b). The estimated parameters assist in scaling the X-ray images and subsequently determine the C-Arm's viewing angle (θ) for each X-ray image (Equations 1 and 2).

$$Scaling\ ratio = \frac{d}{d_{major}}, \tag{1}$$

where, d is the real size of the coin diameter, d_{major} and d_{minor} are the major and minor axes of the ellipse, i.e., coin projection in the image, respectively.

$$\theta = \cos^{-1} \frac{d_{minor}}{d_{major}} \tag{2}$$

C. 2D to 3D transformation

We derive 2D to 3D transformation matrices using defined global coordinate, which correlates a series of X-ray images from different viewing directions. To find the three-dimensional position of a particular point in the global coordinates, we use the relative coordinates of point A in two different images, i.e., (x_1^A, z_1^A), (x_2^A, z_2^A), as shown in Figure 3.a. Since the camera rotates around Y-axis while taking a series of images, Y coordinates remain the same in all the three coordinates, i.e., world coordinate, and relative coordinate in the first and second images ($Y_A = y_1^A = y_2^A$). As mentioned earlier, the relative position of the coin and the bone are fixed when taking images. Therefore, we have no displacement and only need a rotation transformation matrix, as in (3) and (4).

$$\begin{bmatrix} X \\ Z \end{bmatrix} = \begin{bmatrix} cos\,\theta & sin\,\theta \\ -sin\,\theta & cos\,\theta \end{bmatrix} \begin{bmatrix} x_1^A \\ z_1^A \end{bmatrix} \tag{3}$$

$$\begin{bmatrix} X \\ Z \end{bmatrix} = \begin{bmatrix} cos\,\theta & sin\,\theta \\ -sin\,\theta & cos\,\theta \end{bmatrix} \begin{bmatrix} x_2^A \\ z_2^A \end{bmatrix} \tag{4}$$

By rearranging (3) and (4), we obtain (5);

$$\begin{bmatrix} x_1^A \\ z_1^A \end{bmatrix} = R \begin{bmatrix} x_2^A \\ z_2^A \end{bmatrix}, R = \begin{bmatrix} \cos\theta_1 & -\sin\theta_1 \\ \sin\theta_1 & \cos\theta_1 \end{bmatrix} \begin{bmatrix} \cos\theta_2 & \sin\theta_2 \\ -\sin\theta_2 & \cos\theta_2 \end{bmatrix} \tag{5}$$

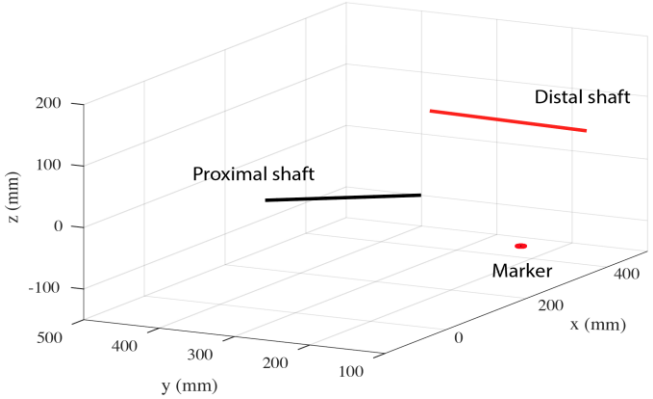

Figure 4. The relative spatial position of the shafts of the main femur fragments.

As a result, we obtain the position of point A in space. Then, using two X-ray images, we find the spatial position of two points A and B on the main axis of the femur, which is the direction of the main axis of the femur in space.

D. Path-Planning Algorithm

After determining the spatial position of the distal and proximal femur shafts, we use the acquired data as an input to our path-planning algorithm. We simulate the integration of the proposed imaging technique with the Robossis, i.e., the innovative surgical robot. A working environment is created to simulate and display real-time physical movements of the bone fragments, which are attached to the robot platforms, with applied forces and constraints. We used SolidWorks to show the robot CAD model and simulate the robot motion. Prior to exporting the SolidWorks assembly into MATLAB, the distal and proximal bones are made concentric to the moving plate as shown in Fig. 5. In addition, SolidWorks mates are simplified to aggregate non-moving parts into rigid bodies and revised for software compatibility.

IV. Preliminary Results

A. Validation of the detected ellipse's parameters

As shown in Figure 3.b, the average error rates of the estimated C-Arm viewing angles at 30°, 45°, and 60° are 13.3%, 3.3%, and 0.8%, respectively. As a result, the developed algorithm offers high accuracy in estimating the parameters of the coin projection at 45° and 60°, while at smaller angles, the thickness of the coin interferes in the results. Therefore, we should use a flat marker to improve the results at a smaller C-Arm angle of view.

B. 3D visualization of the shaft of the main femur fragments

To demonstrate the feasibility of our approach, the developed formula is applied to several pairs of X-ray images of distal and proximal fragments. Figure 4 shows the spatial relative position of the center lines of the proximal and distal bone fragments.

C. Execution of the designed path

With the use of Signal Builder, a demonstration of the 5-step algorithm was simulated on a compound femur fracture. Initially, the bone fragments were plate-centered in SolidWorks before exportation to replicate desired positioning conditions. The simulation began with a final joint bone and backtracked the steps while recording each change in inputs. Then, the steps were reversed to observe the procedure chronologically. This includes (1) extending the distal fragment apart from the proximal fragment in the positive z-axis to avoid bone interference, (2) rotating bone fragments with alpha and beta rotations to make them parallel, (3) aligning the distal fragment with the proximal fragment along the z-axis by displacement in the x-y plane, (4) realigning the distal fragment with the proximal fragment using gamma rotations, and (5) reducing the distal fragment to the proximal fragment in the z-axis (Fig. 5). As a result, the reduction of a fractured femur for anatomic alignment is simulated.

V. Conclusion

In this study, we present a new method for automatically

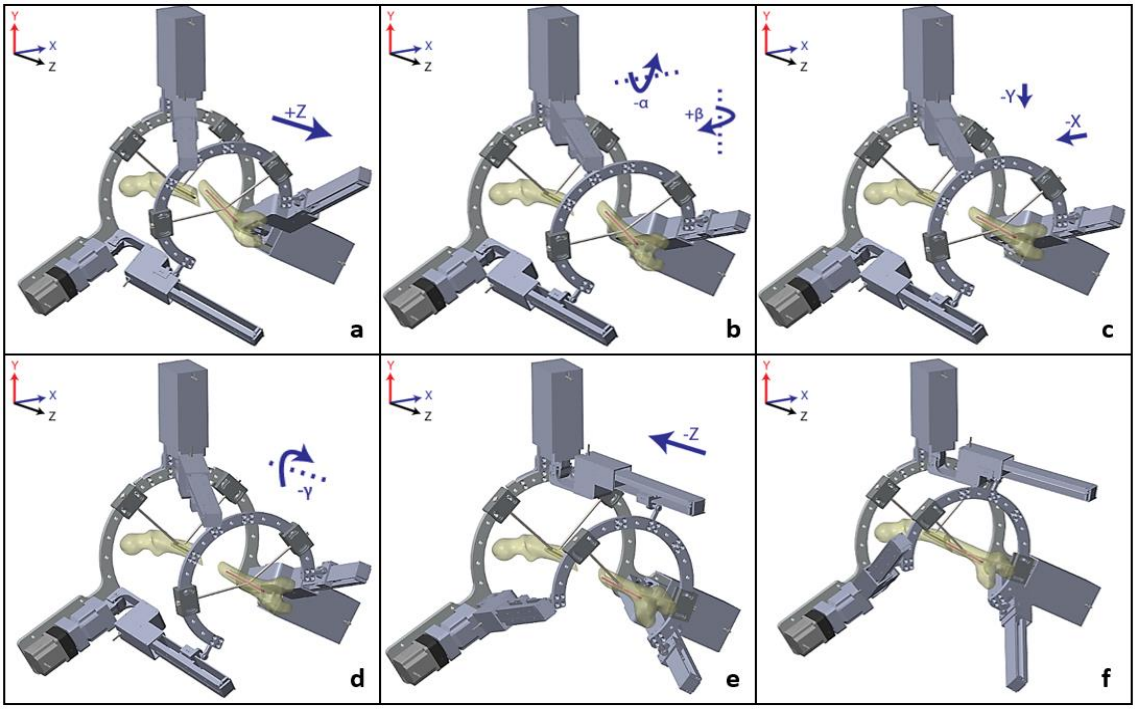

Figure 5. Demonstration of the path-planning algorithm: a) The first position of the fractured femur. b) Step 1- Move interfering bones apart. c) Step 2- Make shafts parallel. d) Step 3- Align shafts on the z-axis. e) Step 4- Correct shaft rotation for alignment. f) Step 5- Bring shafts together, final alignment.

identifying the relative position of the femoral shaft segments in three-dimensional space, for femur fracture reduction surgery. The femoral shaft is one of the main anatomical landmarks used by surgeons to identify the relative position of broken femoral parts in the operating room. To this end, we introduce a marker-based method to connect two-dimensional X-ray images taken from different viewing angles in a three-dimensional coordinate system. Then, using two X-ray images taken from different directions by C-Arm and our derived 2D to 3D transformation equations, we obtain the relative spatial position of the distal and proximal femur shafts. Utilizing our resulting 3D data, we visualize the relative position of the femoral parts, which is a valuable aid to the surgeon during fracture reduction surgery. Besides, we provide a surgical simulation that can help preoperative path planning for femoral fracture alignment. The results of this study facilitate robotic femoral fracture surgery by providing a reliable vision for an innovative surgical robotic system.

REFERENCES

[1] K. J. Agarwal-Harding, J. G. Meara, S. L. M. Greenberg, L. E. Hagander, D. Zurakowski, and G. S. M. Dyer, "Estimating the global incidence of femoral fracture from road traffic collisions: a literature review," JBJS, vol. 97, no. 6, p. e31, 2015.

[2] N. Enninghorst, D. McDougall, J. A. Evans, K. Sisak, and Z. J. Balogh, "Population-based epidemiology of femur shaft fractures," J. Trauma Acute Care Surg., vol. 74, no. 6, pp. 1516–1520, 2013.

[3] J. A. Kaye and H. Jick, "Epidemiology of lower limb fractures in general practice in the United Kingdom," Inj. Prev., vol. 10, no. 6, pp. 368–374, 2004.

[4] J.-W. Kim *et al*., "Malalignment after minimally invasive plate osteosynthesis in distal femoral fractures," Injury, vol. 48, no. 3, pp. 751–757, 2017.

[5] L. Bai, J. Yang, X. Chen, Y. Sun, and X. Li, "Medical robotics in bone fracture reduction surgery: A review," Sensors, vol. 19, no. 16, p. 3593, 2019.

[6] L. Wang *et al.*, "A new hand-eye calibration approach for fracture reduction robot," Comput. Assist. Surg., vol. 22, no. sup1, pp. 113–119, 2017.

[7] T. J. Kovanda, S. F. Ansari, R. Qaiser, and D. H. Fulkerson, "Feasibility of CT-based intraoperative 3D stereotactic image-guided navigation in the upper cervical spine of children 10 years of age or younger: initial experience," J. Neurosurg. Pediatr., vol. 16, no. 5, pp. 590–598, 2015.

[8] N. Baka *et al*., "2D--3D shape reconstruction of the distal femur from stereo X-ray imaging using statistical shape models," Med. Image Anal., vol. 15, no. 6, pp. 840–850, 2011.

[9] S. Zachow, "3D Reconstruction of Anatomical Structures from 2D X-ray Images," 2020.

[10] V. Karade and B. Ravi, "3D femur model reconstruction from biplane X-ray images: a novel method based on Laplacian surface deformation," Int. J. Comput. Assist. Radiol. Surg., vol. 10, no. 4, pp. 473–485, Apr. 2015, doi: 10.1007/s11548-014-1097-6.

[11] N. Hawi *et al*., "Navigated femoral shaft fracture treatment: current status," Technol. Heal. Care, vol. 20, no. 1, pp. 65–71, 2012.

[12] R. Ye, Y. Chen, and W. Yau, "A simple and novel hybrid robotic system for robot-assisted femur fracture reduction," Adv. Robot., vol. 26, no. 1–2, pp. 83–104, 2012.

[13] C. Gosselin and L. T. Schreiber, "Kinematically Redundant Spatial Parallel Mechanisms for Singularity Avoidance and Large Orientational Workspace," *IEEE Trans. Robot.*, vol. 32, no. 2, pp. 286–300, Apr. 2016, doi: 10.1109/TRO.2016.2516025.

[14] M. H. Abedinnasab, F. Farahmand, and J. Gallardo-Alvarado, "The wide-open three-legged parallel robot for long-bone fracture reduction," *J. Mech. Robot.*, vol. 9, no. 1, 2017.

[15] M. H. Abedinnasab, F. Farahmand, B. Tarvirdizadeh, H. Zohoor, and J. Gallardo-Alvarado, "Kinematic effects of number of legs in 6-DOF UPS parallel mechanisms," *Robotica*, vol. 35, no. 12, pp. 2257–2277, 2017.

[16] M. Abedin-Nasab, "Surgical robot," U.S. Patent 10,603,122, 2020.

[17] F.-C. Ghesu *et al.*, "Multi-scale deep reinforcement learning for real-time 3D-landmark detection in CT scans," *IEEE Trans. Pattern Anal. Mach. Intell.*, vol. 41, no. 1, pp. 176–189, 2017.

[18] D. Chudasama, T. Patel, S. Joshi, and G. I. Prajapati, "Image segmentation using morphological operations," *Int. J. Comput. Appl.*, vol. 117, no. 18, 2015.